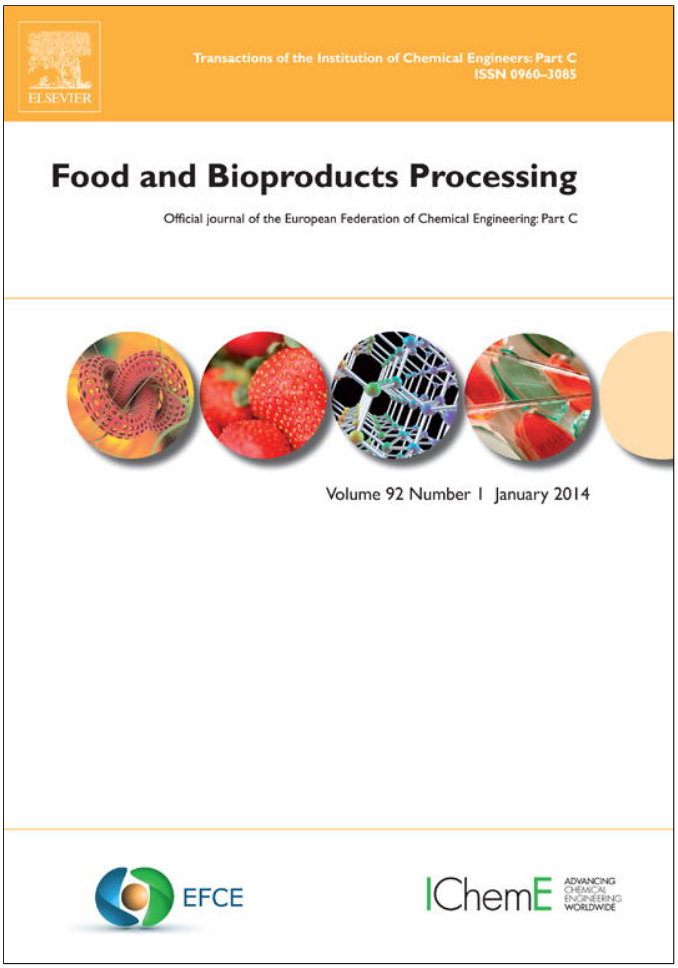

Contents lists available at ScienceDirect

Food and Bioproducts Processing

journal homepage: www.elsevier.com/locate/fbp

Experimental study and numerical modeling of the freezing process of marine products

J.B. Dima[a,b], M.V. Santos[a,c], P.J. Baron[b], A. Califano[a], N.E. Zaritzky[a,c,*]

[a] Centro de Investigación y Desarrollo en Criotecnología de Alimentos-CIDCA, Facultad de Ciencias Exactas, Universidad Nacional de La Plata (UNLP), CONICET, 116 y 47, La Plata (CP 1900), Argentina[1]

[b] Centro Nacional Patagónico (CONICET-CENPAT), Bvard Brown 2825 Puerto Madryn-Chubut, Argentina

[c] Departamento de Ingeniería Química, Facultad de Ingeniería, UNLP, 1 y 47, La Plata, Argentina

ABSTRACT

An increasing interest in the exploitation of new Patagonian marine crabs was manifested by the industry, due to their commercial value as frozen products. In the present work the freezing of two products: crab meat in plastic pouches and crab claws was experimentally conducted and numerically modeled. Non linear, non-stationary heat conduction partial differential equations were solved to simulate the freezing of pouches, using a computational program in finite elements coded by the authors. The freezing of crab claws was simulated considering the irregular geometry of the system and two domains with different thermal properties (crab meat in contact with a calcareous layer) using Heaviside and Gaussian functions, to obtain a smoother specific heat curve. Heat transfer coefficients in the industrial tunnel freezer were determined from independent experiments. The influence of the freezing rate on the size of the ice crystals was determined by histological observations. Numerical models were satisfactorily validated by means of experimental time–temperature curves obtained at industrial scale in freezing tunnels. Tracking of the warmest point paths in each product was performed. These simulations are of great value for food process design and can help to optimize and control the freezing of new products.

Keywords: Marine product; Freezing; Numerical simulation; Crab; Heat transfer; Mathematical modeling

1. Introduction

World exports of processed crab products have increased during the last 20 years. The commercially important species of crustaceans are crabs, lobsters, and shrimps; true crabs are decapod crustaceans of the infra order Brachyura (FAO, 2009). China, United States, Canada, United Kingdom, Thailand, and Russia are among the leading producers of crustaceans. The processing industry of frozen crab meat is an emerging industry in Argentina; presently crab fishing and processing in the Argentine Patagonia (southern South America) has been almost exclusively focused on king crab (*Anomuran*) species (i.e., *Lithodes santolla* and *Paralomis granulosa*). However there is an increasing interest in the exploitation of new species of true crabs due to their abundance and the high commercial value attained in the market. In the coast and shelf off northern and central Argentine Patagonia (42–43°S, 64–65°W) there are two brachyuran crab species recognized as valuable fishing resources (Fenucci and Boschi, 1975; Leal et al., 2008; Dima et al., 2012): the Southern Ocean swimming crab *Ovalipes trimaculatus* and the Patagonian stone crab, *Danielethus* (=*Platyxanthus*) *patagonicus*, recently renamed by Thoma et al. (2012).

Frozen products are one of the main ways in which crabs can be marketed. Crabs must be kept alive at the start of the processing in order to avoid undesirable quality changes in appearance, color, flavor, and texture; they should be cooked immediately after killing (Codex Alimentarius, 1983). Whole crabs must be frozen after cooking since meat is extremely difficult to remove from a crab that has been frozen raw

* Corresponding author at: CIDCA Calle 47 y 116 Fac Cs Exactas, La Plata (1900), Argentina. Tel.: +54 221 4254853; fax: +54 221 4254853.
E-mail address: zaritzkynoemi@gmail.com (N.E. Zaritzky).

Received 12 December 2012; Received in revised form 17 July 2013; Accepted 25 July 2013

[1] http://www.cidca.org.ar/

0960-3085/$ – see front matter
http://dx.doi.org/10.1016/j.fbp.2013.07.012

and subsequently cooked (Edwards and Early, 1976; Codex Alimentarius, 1983). The muscle, or white meat, is removed mainly from the claws, and from the body and legs; the viscera which consists mainly of the digestive gland, or 'liver', and reproductive organs, is removed from the carapace or exoskeleton. King crab (*Lithothes santolla*) is the largest of the commercial crab species and is more suitable for freezing than the other crab species (Codex Alimentarius, 1983). Dungeness crab is frozen as cooked whole or eviscerated crab. Portunid crabs (that includes Blue crabs and *Ovalipes trimaculatus*) are small and not adequate for storing frozen as whole crab; crab meat must be removed from the exoskeleton, packed into plastic bags, heat pasteurized, and then frozen (Gates et al., 1993; Kolbe and Kramer, 2007). Additionally *Danielethus patagonicus* is a *Patagonian* stone crab; this type of crab is recognized by their oval body and two large claws. Stone crabs differ from blue crabs in that only the oversized claws are harvested cooked and frozen (Oshiro, 1999; Alvarez and Briquets, 1983). It is important to accurately predict freezing times of marine foods to assess the quality processing requirements.

The different quality obtained in frozen foods according to whether the freezing is rapid or slow has been subjected to many studies (Fennema et al., 1973; Zaritzky, 2000, 2011). These studies generally consider the different sizes of the ice crystal formed in the tissue as one of the main factors responsible for the changes in quality. The numerical simulation of the heat conduction partial differential equations (PDE) with phase change transition, such as the freezing process, implies that a highly non-linear mathematical problem must be solved, since the thermo-physical properties of the food (thermal conductivity, density, and specific heat) are temperature dependent functions. The abrupt variations of the thermo-physical properties with temperature are due to the conversion of water into ice as the freezing process evolves. The mathematical modeling of food freezing poses special challenges; this subject has been extensively reviewed by Pham (2012).

The numerical solution of PDE governing equations involves two steps: discretizing the space domain to obtain the ordinary differential equations (ODE) relating a finite number of nodal temperatures and then solving this set of ODE by a time stepping method (Pham, 2012). There are three commonly used methods for discretizing space: finite differences (for simple geometries), finite volumes (FVM) and finite elements (FEM); FEM is adequate for shapes that cannot be represented by a regular orthogonal grid.

Usually, in the case of freezing, an apparent specific heat is used, where the latent heat of melting is merged with the sensible heat; therefore this property shows a peak similar to a delta Dirac function. This is due to the release of the latent heat of melting occurring in a very small range of temperature. To circumvent the numerical instabilities that arise when using the finite element method considering variable thermal properties with temperature, transformed variables such as the enthalpy (*H*) and Kirchhoff (E) formulation were used (Scheerlinck et al., 1997, 2001). This formulation is based on the integration of the volumetric apparent specific heat and the thermal conductivity with temperature, respectively (Comini et al., 1974; Mannapperuma and Singh, 1988, 1989; Pham, 2008, 2012). By incorporating these transformed variables in the original heat conduction differential equation a modified and simplified expression is obtained.

Information in literature about mathematical modeling and numerical simulation of the freezing process of marine products of irregular geometry utilizing FEM is scarce. Additionally, in heterogeneous systems, when two or more materials in intimate contact are forming the food structure, such as in the case of crab claws (constituted by muscle and calcareous layer), the enthalpy and Kirchhoff formulations present severe problems such as an inconsistency in the boundary condition because there are different thermal properties, ergo the nodes at the interface have two different H and E values (Pham, 2008, 2012), instead of one single value.

Generally, commercial software based on the finite element method are unable to run and/or converge to accurate temperature predictions when trying to simulate a phase change process due to abrupt changes in the thermo-physical properties, specifically when using the apparent specific heat method. There is limited information in the literature focused on numerical simulations of phase change problems in heterogeneous systems having thermal resistances in series such as in crab claws where meat is in contact with the calcareous exoskeleton; therefore it is necessary to improve mathematical techniques to overcome this problem.

The prediction of accurate processing times is of key importance (Erdogdu, 2010) in order to estimate the energy requirements and the correct design and control of the equipment necessary for the freezing of foodstuffs. The significance of the present study is to provide useful information in order to control and optimize the freezing process of new marine products with high commercial value. Besides, this work contributes to improve the mathematical modeling of the freezing in heterogeneous complex foodstuffs, overcoming the lack of convergence in nonlinear problems.

The objectives of the present work were: (a) to develop a mathematical model and to numerically simulate the freezing process in pouches containing crab meat from *Ovalipes trimaculatus* using a computational program in FEM coded by the authors; (b) to numerically simulate the freezing process in crab claws of *Danielethus (=Platyxanthus) patagonicus* taking into account the irregular geometry and thermal resistances in series represented by two domains with different thermal properties: crab meat in contact with the external calcareous layer of calcium carbonate. In order to implement the model, heat transfer coefficients were experimentally determined using an industrial equipment and Differential Scanning Calorimetry was used to determine key thermal properties; (c) to carry out freezing experiments with Patagonian marine crab products in order to validate the numerical models with experimental results of time–temperature data obtained from industrial scale freezing tunnels; (d) to assess the effect of freezing times on the size and location of the ice crystal sizes in meat tissue; (e) to apply the validated model to track the warmest point paths of each system and to analyze the effect of different operating conditions (external cooling temperatures, surface heat transfer coefficients, initial temperatures) on freezing times of crustaceous products in order to design and control the industrial process.

2. Materials and methods

2.1. Sample preparation

Specimens of the Southern Ocean swimming crab *Ovalipes trimaculatus* (Fig. 1a) and the Patagonian stone crab *Danielethus*

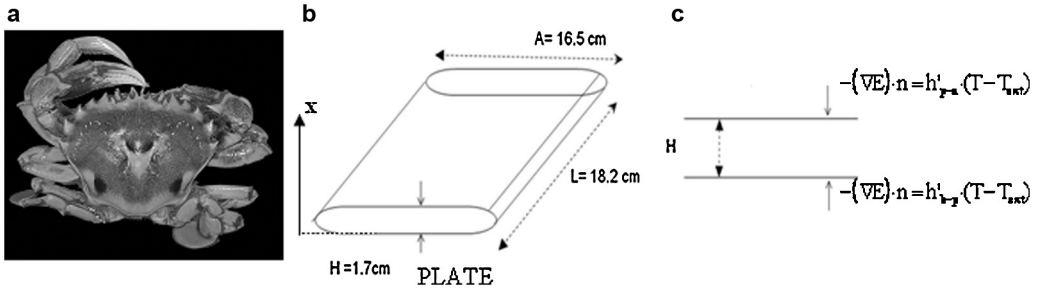

Fig. 1 – (a) Photograph of *O. trimaculatus* crab; (b and c) dimensions of the pouches and geometry used to represent the food system (1D).

patagonicus (Fig. 2a) were collected manually on the sea bottom by scuba diving or captured with baited traps in Golfo Nuevo, Patagonia-Argentina at depths ranging within 0–55 m on board a 4.5-m long semi-rigid boat. Only male crabs larger than 70 mm of carapace width were used in the experiments. The crabs were transported alive to the laboratory within 30 min after capture, where carapace width and manus (i.e., palm) length of both claws were measured with a digital caliper to the lowest 0.1 mm. After that, carapace and viscera were removed from the body; crabs were sectioned and separated in body and claws, and then both parts were exposed to thermal treatment. Thermal treatment experiments were carried out for the detachment of the meat from the crab calcareous layer. Body and claws were thermally treated by immersion in boiling water at 100 °C, for 10 min for the bodies of *O. trimaculatus* and for the claws of *D. patagonicus* (Dima et al., 2012). After cooking, crab pieces were submerged in iced water to stop the thermal process; at this stage crab claws were ready to be frozen. In the case of the bodies this procedure facilitates meat detachment from the exoskeleton; meat from the crab bodies was picked manually, using steel devices. The extracted meat was immediately packed into vacuum plastic pouches (polyethylene, 90 μm thickness) and then pasteurized. Pasteurization was carried out by immersion in thermostatic water bath at 82 °C for 20 min. Finally pouches were submitted to tunnel freezing.

2.2. *Freezing experiments*

Experimental measurements of the thermal histories in pouches and crab claws during freezing were carried out; in all cases experiments were performed at least in triplicates. Different experiments were used to validate the numerical simulations. The meat removed from *Ovalipes trimaculatus* was packed into plastic pouches. Fig. 1b and c show a schematic view of the crab pouches and the geometry used to represent this food system.

Claws of *Danielethus patagonicus* crab (Fig. 2a and b) constitute a system of two domains with different thermo-physical properties; crab meat and an external calcareous layer. The

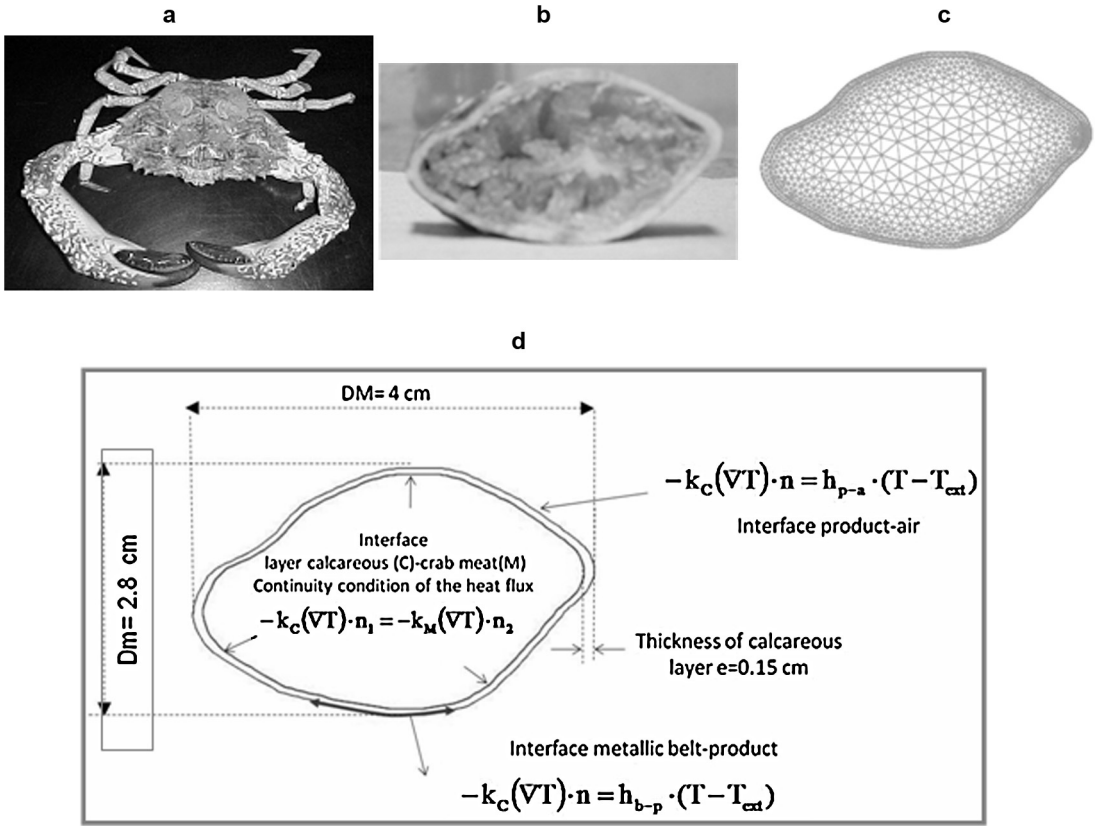

Fig. 2 – (a) Photograph of *D. patagonicus* crab; (b) digital image of the cross section of a crab claw; (c) mesh used to discretize both domains; (d) characteristic dimensions and boundary conditions used in the bidimensional model.

length of the claws of *D. patagonicus* ranged between 0.090 and 0.125 m. The axes of the cross sections of the claws ranged between 0.037 and 0.048 m (major axis) and 0.027–0.035 m (minor axis).

Samples of crab meat pouches and claws were frozen in an industrial tunnel freezer 6 m long with a cross sectional area of 3.6 m^2 designed by Refmar S.R.L., in a plant located in Puerto Madryn, Chubut, Argentina. The conveyor belt freezer operated continuously having six blowers at the upper section. The minimum cooling temperature of the tunnel was −40 °C and the maximum residence time of the samples was 40 min. The air velocity was recorded with a portable digital anemometer (Model ST82, Standard Instruments Co, China). The average air velocity in the tunnel freezer was 4.16 m/s for a frequency air blower of 40 Hz. Freezing of pouches and claws were carried out on a metal belt inside the tunnel; the air was forced to circulate at different velocities by the air blowers. Calibrated thermocouples type K connected to an acquisition device recorded the time–temperature data inside the claws. Also the external air temperature was recorded during all the experiments. In the case of plastic pouches since the insertion of a thermocouple implicated loss of vacuum in the package, a wireless device type data logger of reduced size was used (iButton® Sensors, Maxim products USA). The working temperature range of the device is −55 °C to 100 °C and the temperature data was recorded every 1 min. The small sensor was placed at the geometric center of the pouches.

2.3. Determination of the thermo-physical properties

2.3.1. Proximate composition

In order to determine the thermo-physical properties of crab meat, moisture, protein, fat, carbohydrates, and ash content in body and claw muscle were analyzed for both species of crustaceous. Moisture content was determined by drying the sample in an oven at 105 °C to constant weight (AOAC, 1990). Crude protein content was determined by the Kjeldahl method (AOAC, 1990), using a conversion factor of 6.25 to convert total nitrogen to crude protein. Fat was determined by using the Soxhlet extraction method (AOAC, 1990). Ash content was obtained by ashing the samples in a furnace at 550 °C for 8 h (AOAC, 1990). Carbohydrates were determined by difference. All analyses were conducted in triplicate.

2.3.2. Initial freezing temperature

The initial freezing temperature *Tf* was experimentally determined from the freezing curves. *Tf* was measured by using thermocouples inserted in the crab meat samples by applying the tangent method (Fennema et al., 1973).

2.3.3. Experimental measurements by differential scanning calorimetry (DSC)

Specific heat and latent heat of ice melting of the crab meat were measured by using a differential scanning calorimeter (DSC) TA Instruments, New Castle, Delaware, USA model Q100 controlled by a TA 5000 module with a quench cooling system under a nitrogen atmosphere at 20 mL/min. Samples of crab meat were enclosed in sealed aluminum pans. An empty pan was used as a reference sample. Pans were heated at 10 °C/min from −50 to 100 °C with isothermal periods at the initial and final temperatures. In order to measure the specific heat three scans were made: one for the sample, one for a standard (sapphire), and one for the empty sample pan. In these scans the reference holder contains an empty pan. Distilled water was also scanned using the same program to verify the equipment calibration. The specific heat was calculated following the ASTM E1269 (2003) procedure and McNaughton and Mortimer (1975) recommendations.

The latent heat of melting (ΔH_m) was determined as indicated by Roos (1986) by integrating the peak of the melting curve; this value was used to estimate the unfrozen water fraction in the food material. The temperature integration limits of the peak were chosen when a clear separation between curve and base line was detected.

Unfrozen water (*xb*), was considered as the difference between total water content and the amount of frozen water in the deep frozen material. The mass fraction of frozen water was obtained from the ratio between the latent heat of melting determined for the food material and the heat of melting of pure water.

2.3.4. Ice content as a function temperature

The ice content as a function temperature (at $T < Tf$) was estimated using the equation proposed by Miles et al. (1983):

$$xh = (x_{wo} - xb)\left(1 - \frac{Tf}{T}\right) \quad (1)$$

where *xh* is the mass fraction of ice, *Tf* and *T* are given in °C, x_{wo} is the total mass fraction of water in the sample. The value of *xb* was experimentally determined using DSC measurements.

2.4. Determination of the heat transfer coefficients

Experiments were carried out to determine the heat transfer coefficients (*h*) during the freezing process of crab claws ($h_{p\text{-}a}$ at the air-crab claw interface and $h_{b\text{-}p}$ at the interface between the belt and the product) and meat pouches (h'_{p-a} at the interface pouch-air and h'_{b-p} at the interface belt-pouch).

Aluminum bodies (spheres, cylinders and prisms) in which a thermocouple type K was inserted at the geometric center were used to determine the heat transfer coefficients in the case of claws and pouches, respectively. Time–temperature curves were recorded during the cooling process of these metallic bodies in the tunnel freezer, submitted to the same operating conditions as those of the crab claws and pouches.

In order to estimate $h_{p\text{-}a}$ and h'_{p-a} the metal objects were kept separated from the metal belt by placing them over perforated polystyrene supports to allow the cooling air to circulate through the surrounding object. Once $h_{p\text{-}a}$ and h'_{p-a} were determined, the evaluation of $h_{b\text{-}p}$ and h'_{b-p} was performed from the time temperature curves of the aluminum objects placed over the conveyor belt.

All the experiments were performed at least in triplicates for each condition. Different heat transfer coefficients were proposed in the numerical solution; the experimental thermal histories were compared with the numerical simulations and the heat transfer coefficient that minimized the residual sum of squares (squared differences between the experimental and predicted temperatures) was selected.

It must be pointed out that independent experiments were carried out to determine the heat transfer coefficients and to validate the model.

2.5. Histological analysis

To assess the effect of freezing rates on the size and location of the ice crystals in the frozen crab tissue a histological

technique was applied based on the freeze substitution method, whereby observations were made of the holes left by the ice crystals in the tissue (Bevilacqua et al., 1979; Bevilacqua and Zaritzky, 1980; Martino and Zaritzky, 1989).

In the isothermal freeze fixation small samples of (0.5 cm. diameter and 0.5 cm. thickness) of the tissue were fixed at the final freezing temperature using Carnoy fluid (absolute ethyl alcohol 60%, chloroform 30% and glacial acetic acid 10%, v/v). The fixative has a low freezing point, it diffuses and penetrates in the tissue and simultaneously ice crystals are dissolved maintaining their contours. Once the tissue was fixed, samples were brought to room temperature, dehydrated using a series of gradually increasing concentrations of ethyl alcohol, cleared in toluene, and embedded in paraffin (56–58 °C). Sections of the samples (8–10 μm) obtained by a rotary microtome were mounted on glass slides and stained with hematoxylin–eosin for histological examination. Micrographs of the specimens were obtained with a Zeiss microscope with a digital camera coupled to an Image Analysis software (Martino and Zaritzky, 1989).

Micrographs were associated to the local characteristic freezing time (tc) of a given point, that is defined as the time necessary for this point to pass from the initial freezing temperature to −10 °C. This time interval was determined from the experimental time–temperature curves recorded by the thermocouples inserted in the tissue; local freezing time is inversely correlated with the freezing rate in a given point of the sample (Bevilacqua et al., 1979; Bevilacqua and Zaritzky, 1980).

3. Mathematical modeling and calculation

The numerical technique to solve the heat transfer partial differential equation was based on the finite element method. A code develop by the authors using Matlab language was applied in the case of crab meat packed in plastic pouches using the enthalpy and Kirchhoff formulation, and a commercial software (COMSOL Multiphysics) was used in the case of crab claws.

3.1. *Freezing of pouches*

The heat conduction equation in terms of the temperature variable is:

$$\rho(T)Cp(T)\frac{\partial T}{\partial t} = \nabla\cdot(k(T)\nabla T) \tag{2}$$

Considering the following transformation of variables:

$$H(T) = \int_{T^*}^{T} \rho(T)\cdot Cp(T)\,dT \tag{3}$$

$$E(T) = \int_{T^*}^{T} k(T)\,dT \tag{4}$$

where H is defined as the volumetric enthalpy obtained by integration of the volumetric specific heat with temperature, and E is the Kirchhoff function represented by the integral of the thermal conductivity with temperature. These functions are monotonic increasing and continuous because Cp, k, and ρ are positive and bounded. Consequently, there exists a one to one mapping between the enthalpy/Kirchhoff values and the temperature variable. T^* (one of the limits of integration) is a reference temperature corresponding to a zero value of enthalpy and Kirchhoff function.

The initial and boundary conditions are as follows:

$$T = T_0, \quad t = 0 \quad \text{in} \quad \Omega \tag{5}$$

$$-k\left(\frac{\partial T}{\partial x}\cdot n_x + \frac{\partial T}{\partial y}\cdot n_y + \frac{\partial T}{\partial z}\cdot n_z\right) = h'_{b-p}(T - T_{ext}), \quad t\geq 0 \quad \text{in} \quad \delta\Omega_{b-p} \tag{6}$$

$$-k - \left(\frac{\partial T}{\partial x}\cdot n_x + \frac{\partial T}{\partial y}\cdot n_y + \frac{\partial T}{\partial z}\cdot n_z\right) = h'_{p-a}(T - T_{ext}), \quad t\geq 0 \quad \text{in} \quad \delta\Omega_{p-a} \tag{7}$$

where the subscript "$b-p$" corresponds to the interface belt-product and "$p-a$" to product-air. In the boundary condition described by Eq. (6) the heat transfer coefficient (h'_{b-p}) represents the film thermal resistance of the pouch containing the crab meat in contact with the metal plate. In Eq. (7), h'_{p-a} includes the heat transfer coefficient of the cooling air and the thermal resistance of the pouch plastic film.

Combining Eqs. (2)–(4) with the initial and boundary conditions represented in Eqs. (5)–(7) the following strong formulation is obtained in terms of Enthalpy variable (Santos et al., 2010):

$$\frac{\partial H}{\partial t} = \nabla^2 E \quad \text{in} \quad \Omega, \quad t\geq 0 \tag{8}$$

$$-(\nabla E)\cdot n = h'_{b-p}\cdot(T - T_{ext}) \quad \text{in} \quad \delta\Omega_{b-p}, \quad t\geq 0 \tag{9}$$

$$-(\nabla E)\cdot n = h'_{p-a}\cdot(T - T_{ext}) \quad \text{in} \quad \delta\Omega_{p-a}, \quad t\geq 0 \tag{10}$$

$$H = H_0, \quad t = 0 \tag{11}$$

Defining the residual as:

$$r = \frac{\partial H}{\partial t} - \nabla^2 E \tag{12}$$

Applying the weight residual method:

$$\int_{\Omega} N^T\left(\frac{\partial H}{\partial t} - \nabla^2 E\right)\,d\Omega = 0 \tag{13}$$

Using the differential rule the term $-N^T\nabla^2 E$ can be written as $-\nabla\cdot(N^T\nabla E) + \nabla N^T\cdot\nabla E$. Then, after incorporating the divergence theorem:

$$\int_{\Omega} N^T\frac{\partial H}{\partial t}\,d\Omega - \int_{\delta\Omega} N^T\nabla E\cdot n\,d\delta\Omega + \int_{\Omega}\nabla N^T\cdot\nabla E\,d\Omega = 0 \tag{14}$$

The boundary conditions Eqs. (9) and (10) are incorporated in the variational formulation in the second term of Eq. (14) obtaining:

$$\int_{\Omega} N^T\frac{\partial H}{\partial t}\,d\Omega + \int_{\delta\Omega_{plate-p}} N^T h'_{b-p}(T - T_{ext})\,d\delta\Omega + \int_{\delta\Omega_{p-a}} N^T h'_{p-a}(T - T_{ext})\,d\delta\Omega + \int_{\Omega}\nabla N^T\cdot\nabla E\,d\Omega = 0 \tag{15}$$

Reorganizing the equation and implementing the Galerkin method:

$$CG \cdot \frac{dH}{dt} + FG \cdot T(H) + KG \cdot E(H) = m \quad (16)$$

where $CG = \sum_{e=1}^{ne} \int_{\Omega_e} (N^T N)\, d\Omega_e$ is the global capacitance matrix; $KG = \sum_{e=1}^{ne} \int_{\Omega_e} (B^T B)\, d\Omega_e$ is the global conductance matrix; $FG = \sum_{s=1}^{ns1} \int_{\Omega_s} (N^T h'_{b-p} N)\, d\delta\Omega_s + \sum_{s=1}^{ns2} \int_{\Omega} (N^T h'_{p-a} N)\, d\delta\Omega_s$ is the global convective matrix; $m = \sum_{s=1}^{ns1} \int_{\delta\Omega_s} (N^T h'_{b-p} T_{ext})\, d\delta\Omega_s + \sum_{s=1}^{ns2} \int_{\delta\Omega_s} (N^T h'_{p-a} T_{ext})\, d\delta\Omega_s$ is the global force vector; H, E, and T are the nodal enthalpy, Kirchhoff and temperature values, respectively.

It can be observed that the thermal properties of the foodstuffs have been incorporated into the new mathematical formulation as dependent variables; H, E, and T vary with the position of the node and with time.

The matrices KG, FG, CG and the vector m contain only information about the interpolation functions and heat transfer coefficients, reducing the computation time significantly. The advantage of the Enthalpy method is that instead of solving the original partial differential equations using the temperature as a variable, the problem was reformulated into another partial differential equation which uses an Enthalpy variable that varies with position and time. However the matrices KG, FG, CG, that do not contain information on the thermal properties, remain constant. It must be emphasized that this methodology takes into account the variation of the properties $Cp(T)$, $\rho(T)$ and $k(T)$, with position, temperature and time as the freezing process occurs. When implementing the variational formulation using the finite element method the problem to be solved is simplified and can be represented as a System of Ordinary differential Equations giving a solution in terms of enthalpy values over the entire domain and as a function of position of the node and time.

Eq. (16) is a system of ordinary differential equations with three unknown variables, H, E, and T that are interrelated through non-linear algebraic functions, $H(T)$, $E(T)$, $H(E)$, $T(H)$, $T(E)$, and $E(H)$. The temperature dependence of the thermal properties are incorporated into the enthalpy formulation by using this $T(H)$ and $E(H)$ functions. First the $H(T)$ and $E(H)$ were constructed according to Eqs. (3) and (4) with the $Cp(T)$ and $k(T)$ integrals. Next using Matlab 6.5 piece-wise interpolating functions the $T(H)$ and $E(H)$ functions were obtained. Incorporating the functions $E(H)$ and $T(H)$ into Eq. (16) the system can be rewritten as (Santos et al., 2010; Santos and Lespinard, 2011):

$$\frac{dH}{dt} = f(H) \quad (17)$$

The system was solved using the standard Matlab 6.5 routines ODE (Ordinary Differential Equations) where the enthalpy values at each node are calculated for each time step. The temperature distribution was obtained using the function $T(H)$, previously determined. As a result, the temperature over the domain can be estimated using the interpolating function used in the finite element technique (Santos et al., 2010; Santos and Lespinard, 2011).

The dimensions of the crab meat pouches allow the system to be considered as a one dimensional heat transfer problem, being the most important shape factor the thickness of the crab meat. Therefore Eq. (9) corresponds to the boundary condition at x = 0 and Eq. (10) to $x = 1.7$ cm (Fig. 1b).

3.2. *Freezing of crab claws*

The crab claw geometry was considered as an irregular bi-dimensional object, the axial heat flow was considered negligible in comparison to the transverse energy contribution. The finite element meshes were generated using the irregular contours of the cross-sectional image. These figures were then imported into the COMSOL program using an image capturing program that used functions implemented in Matlab language. At first the image was transformed from a color RGB to a BW (black and white) format in order to enhance the contrast of the picture and have a defined contour of the cross sectional geometry. Then using a built in Matlab function called "flim2curve" a specific number of points from the contour curve were captured and converted into a solid domain that was then exported into COMSOL environment for the mesh generation. Fig. 2b shows a cross section of a claw and Fig. 2c shows the spatial discretization of the domain using triangular elements of order 2. The mathematical problem was solved taken into account the 2D irregular contour at the half section of the claw (Fig. 2d).

The crab meat suffers phase change during freezing however the calcareous layer properties remain constant during the entire temperature range. The equations that describe the process are:

$$\rho_M(T) Cp_M(T) \frac{\partial T}{\partial t} = \nabla \cdot (k_M(T) \nabla T) \quad \text{in} \quad \Omega_M \quad (18)$$

$$\rho_C Cp_C \frac{\partial T}{\partial t} = \nabla \cdot (k_C \nabla T) \quad \text{in} \quad \Omega_C \quad (19)$$

where the subscripts "M" and "C" correspond to the crab meat and the calcareous layer, respectively.

The initial and boundary conditions are the same as those described in Eqs. (5)–(7), applied to a bi-dimensional problem with 2 domains considering a heat transfer coefficient in the zone where the claw is in contact with the metallic belt ($h_{b\text{-}p}$) and the heat transfer coefficient in the zone exposed to the cooling air over the product ($h_{p\text{-}a}$).

Digital images of each sample were processed in order to obtain the irregular contours and domains of each material; this information was imported into the software to generate the triangular mesh and nodes (Fig. 2c).

As explained before the problem of having two different materials with different thermo-physical properties in perfect contact makes the enthalpy and Kirchhoff formulation to be inapplicable, since there are two values of E and H at the interface of both materials (Pham, 2008). In this case, the software COMSOL Multiphysics was used to simulate the heat transfer problem with phase change taking into account that both thermal resistances (calcareous layer and crab meat) are in series. To overcome the abrupt variation of the apparent specific heat (Cp) with temperature, the method used was based on representing Cp as the sum of a Heaviside and Gaussian functions, generating a smoother curve around the phase change temperature range (COMSOL Multiphysics 2012, Neeper, 2000). In this way the numerical instabilities in the finite element resolution were avoided and the finite element program was able to deal with the marked change in the Cp function without modifying important physical values such as phase change temperature range, peak temperature, and latent heat of melting.

3.3. Statistical analysis

Experiments to validate de numerical models using plastic pouches and crab claws were performed at least in triplicates. The root-mean-square error (RMSE) was used to measure the differences between predicted ($T_{numerical}$) and experimental temperatures (T_{exp}) for each experiment. Moreover, the maximum absolute deviation, infinite norm, L^{∞} (MAD $= \max|T_{exp} - T_{numerical}|$) was also calculated.

Statistical analysis and polynomial regressions were performed by using the software SYSTAT 12 (Systat Software Inc.).

4. Results and discussion

4.1. Thermophysical properties

4.1.1. Proximate composition and initial freezing temperature

The chemical composition of the crab meat was experimentally obtained: $x_{water} = 0.770$, $x_{carbohydrate} = 0.051$, $x_{fat} = 0.005$, $x_{protein} = 0.160$, $x_{ash} = 0.014$ (mass fraction, wet basis).

The initial freezing (Tf) temperature measured using the Tangent method was −1.7 °C.

4.1.2. Experimental data obtained by DSC

The latent heat of ice melting of the crab meat was $\Delta H_m = 243{,}350$ J/kg. The unfrozen water (mass fraction, wet basis) was $xb = 0.1484$, specific heat of the crab meat at a fully frozen state (measured at −35 °C) was $Cp_{fc} = 1894.3$ J/kgK, and the specific heat of the unfrozen crab measured at a temperature above Tf ($T = 10$ °C) was $Cp_{ufc} = 3848.3$ J/kgK.

4.1.3. Thermal conductivity and density

As was reported in Carson (2006) it is difficult to give comprehensive generic guide lines for predicting the thermal conductivity for Class II foods (nonporous frozen foods). Values of thermal conductivities reported by Wang and Curtis (2012) and Ahmed and Rahman (2009) were in the range 1.3–1.5 W/m K in the range (−20 to −10 °C) with initial water contents of 77% wet basis. The Maxwell Eucken gave an asymptotic value of k at −40 °C (fully frozen state) of 1–1.2 W/m K, which is lower than the experimental data. In contrast the Choi and Okos (1986) model was in agreement with experimental data found in the literature and provided excellent results when the numerical model was validated against experimental time-temperature curves.

Therefore the thermal conductivity of the crab meat was calculated using Choi and Okos (1986) equation as follows:

$$k(T) = \sum x_i^v \cdot k_i(T) \tag{20}$$

where k is the global conductivity, given in W/m K, k_i is the thermal conductivity (W/m K) of the component i, where i corresponds to the different components: water, ice (if the temperature is lower than the initial freezing temperature Tf), carbohydrate, fat, etc. and x_i^v corresponds to the volumetric fraction of each component.

The density of the crab meat was calculated using the following equation (Choi and Okos, 1986):

$$\rho(T) = \frac{1}{\sum x_i/\rho_i} \tag{21}$$

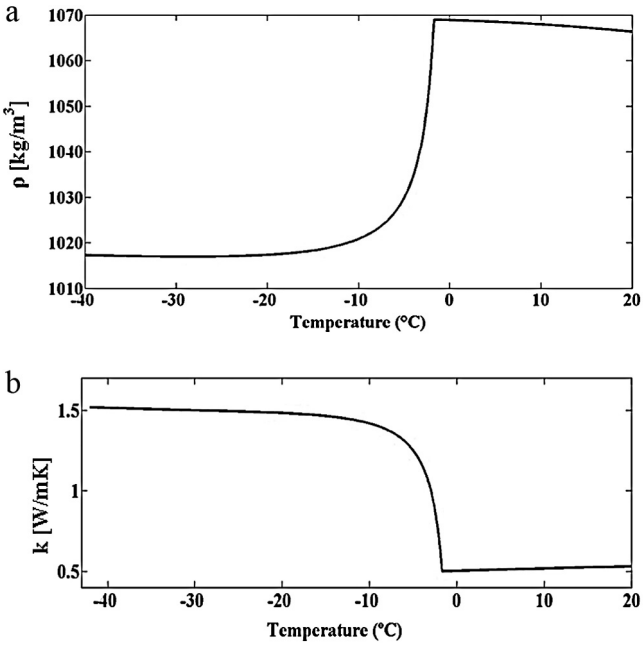

Fig. 3 – Properties of crab meat as functions of temperature: (a) density; (b) thermal conductivity.

where $\rho(T)$ is the global density and ρ_i is the density of the component i (where i corresponds to the different food components, as previously explained) and x_i corresponds to the mass fraction of each component.

The thermal conductivity and density as functions of temperature were estimated by incorporating the experimental data of proximate composition, initial freezing temperature, unfrozen water content into equations (Eqs. (20) and (21)). Results are shown in Fig. 3a and b.

4.1.4. Specific heat, enthalpy and Kirchhoff functions used in the simulations of freezing of crab meat in plastic pouches

In the case of crab meat the apparent specific heat was estimated using the equation proposed by Miles et al. (1983):

$$Cp(T) = \sum x_i Cp_i - Lx_w \frac{Tf}{T^2} \tag{22}$$

where L is the latent heat of melting of water (333.6 kJ/kg); Tf is the initial freezing temperature (in °C) experimentally determined; Cp is the global specific heat; Cp_i is the specific heat of component i (where i corresponds to the different food components: water, ice (if the temperature is lower than the initial freezing temperature Tf), carbohydrate, fat, etc.).

Apparent specific heat of crab meat calculated by using Eq. (22) is shown in Fig. 4a.

Once the thermo-physical properties of crab meat (Cp, k, and ρ as a function of temperature) were obtained, the enthalpy and Kirchhoff functions vs. temperature were calculated by using Eqs. (3) and (4).

The volumetric Enthalpy was calculated by integrating the volumetric specific heat ($\rho(T) \times Cp(T)$) curve with temperature (Fig. 4b). The Kirchhoff function was obtained by integrating the $k(T)$ function with temperature (Fig. 4c). These functions were incorporated in the finite element program coded in Matlab language in order to simulate the freezing process in plastic pouches.

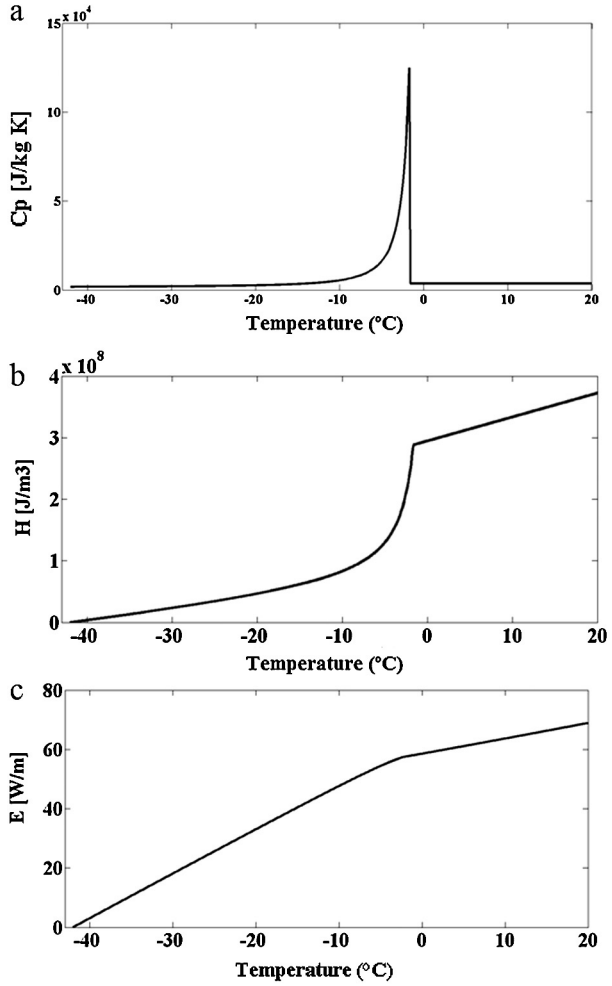

Fig. 4 – Effect of temperature on thermal properties of crab meat: (a) apparent specific heat using Eq. (22); (b) enthalpy; (c) Kirchhoff function.

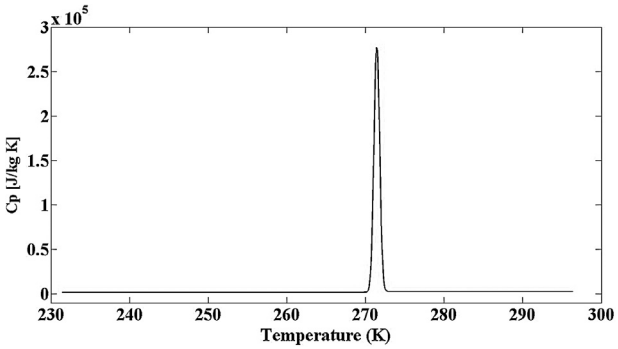

Fig. 5 – Apparent specific heat of crab meat using Heaviside and Gaussian functions (Eqs. (23) and (24)).

4.1.5. *Thermal properties used for crab claws simulations*

The properties (k, ρ, Cp) of both materials of the crab claws, the calcareous layer and crab meat, were used in the commercial software. Crabs are arthropods whose carapace is comprised of a mineralized hard component, mostly calcium carbonate (calcite), and a softer organic component, which is primarily chitin. In crustaceans, such as crabs, there is a high degree of mineralization; the mineral which deposits onto the space of chitin-protein network gives rigidity to the exoskeleton (Meyers et al., 2008). The thermal conductivity, density and specific heat of the calcareous layer were: $k = 3.89$ W/m K (Midttomme et al., 1998; Brigaud and Vasseur, 1989), $\rho = 2700$ kg/m^3 (Green and Perry, 2007), $Cp = 806.62$ J/kg K (Jacobs et al., 1981).

For the crab claw meat a sum of two functions, Heaviside and Gaussian functions, were used to obtain a smother function of the specific heat with temperature as follows:

$$Cp_c(T) = Cp_{fc} + \frac{\Delta H_m}{Tm} \cdot f(H_{ea}) + D \cdot \Delta H_m \quad (23)$$

where Cp_{fc} is the specific heat of the crab meat at a fully frozen state, Tm is the peak temperature curve (equivalent to the mean value μ in the Gaussian curve), ΔH_m is the latent heat of melting of the food, and D is the Gaussian function defined as:

$$D(T) = \frac{e^{(-(T-T_m)^2/dT^2)}}{\sqrt{\pi dT^2}} \quad (24)$$

where dT is the half transition range, $2dT$ is the temperature range where 84% of the latent heat of melting is released (Neeper, 2000), $f(H_{ea})$ is the Heaviside step function. This is a built-in function in the Comsol-Matlab environment and it has the excellent advantage that it gives second order continuous derivatives to the Cp function. A similar approach based on the application of smoothed Heaviside functions with continuous derivative was used by Purlis (2011) to incorporate the phase transition into thermo-physical properties of bread baking.

Eqs. (23) and (24) were calculated incorporating the experimental data obtained by DSC measurements, $\Delta H_m = 243{,}350$ J/kg and $Cp_{fc} = 1894.3$ J/kgK, considering a $dT = 0.5$ °C; and a peak temperature $Tm = -1.7$ °C. Fig. 5 shows the $Cp(T)$ curve used in the commercial software.

4.2. *Heat transfer coefficients*

The heat transfer coefficients that best fitted the experimental data for pouches were h'_{p-a} (product-air) = 10 W/m^2 K and h'_{b-p} (belt-product) = 80 W/m^2 K. The heat transfer coefficients for crab claws that best fitted all the experimental data were $h_{p\text{-}air} = 20$ W/m^2 K and $h_{b\text{-}p} = 500$ W/m^2 K.

4.3. *Model validation: comparison of the numerical simulations and freezing experiments*

Fig. 6 shows an example of the experimental average temperatures during freezing of crab packed in plastic pouches and the predicted temperatures vs. time curve obtained by the numerical model developed in Matlab language. The conditions of the experiments shown in Fig. 6 were: initial temperature $T_i = 7$ °C, air temperature $T_{ext} = -40$ °C; thermocouple position = 0.85×10^{-2} m (center of the pouch). The accuracy of the temperature sensors was ±0.5 °C; the tests were performed in triplicates and the standard error of the mean experimental temperatures was represented by the error bar shown on the top of the Fig. 6a.

The values of the heat transfer coefficients were those reported in Section 4.2.

The accuracy of the numerical models was confirmed by comparison of the average experimental time–temperature

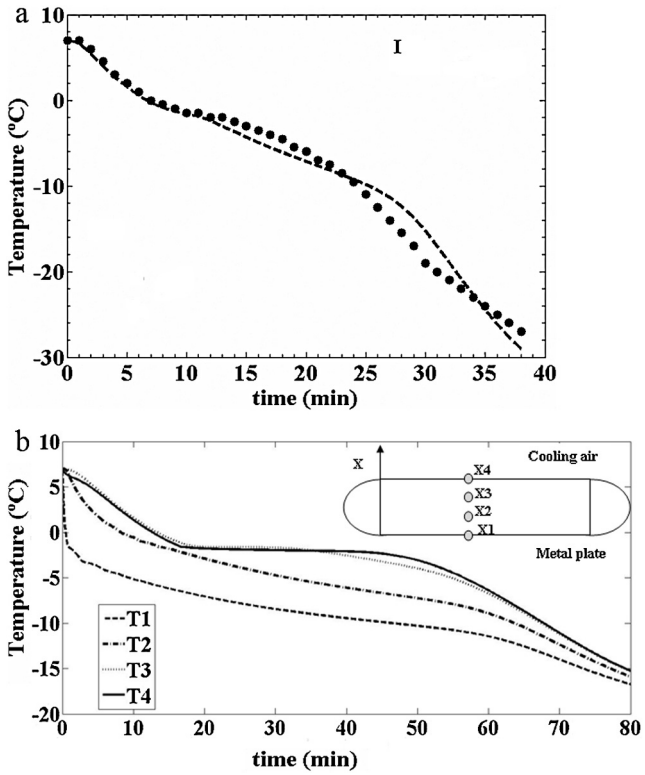

Fig. 6 – (a) Freezing of crab meat in plastic pouches. (●) Average experimental temperatures; (—) predicted temperatures by the numerical model using enthalpy and Kirchhoff formulation. *Experimental conditions*: $T_i = 7\,°C$, $T_{ext} = -40\,°C$, h'_{p-a} (product-air) $= 10\,W/m^2\,K$, h'_{b-p} (belt-product) $= 80\,W/m^2\,K$, thermocouple position $= 0.85 \times 10^{-2}$ m (center of the pouch). Error bar on the top of the figure represents the standard error of the mean experimental temperatures. (b) Temperature predictions for different positions in the pouch X1 = 0 m, X2 = 0.0057 m, X3 = 0.0125 m, and X4 = 0.0170 m. T1, T2, T3, and T4 correspond to the temperature predictions for X1, X2, X3, and X4, respectively.

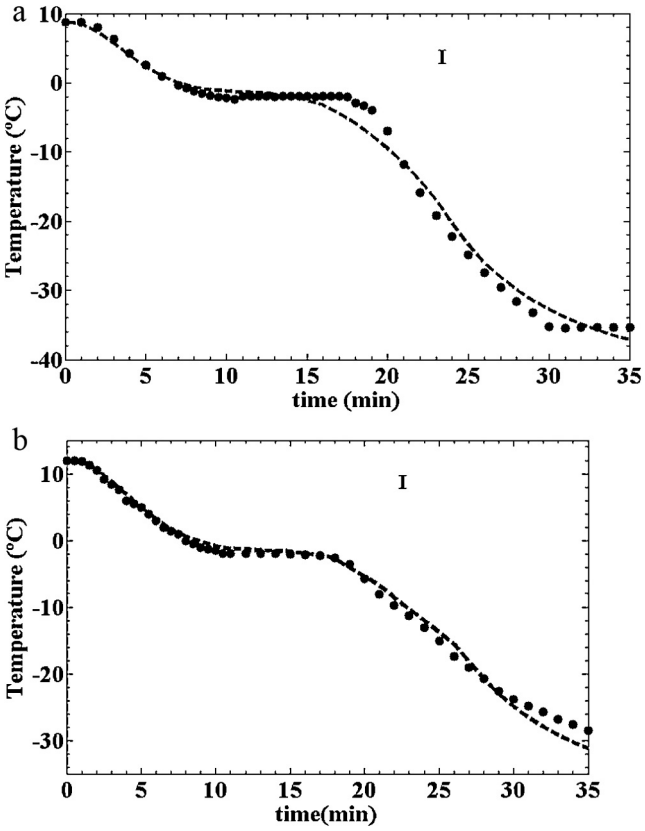

Fig. 7 – Freezing of crab claws. (●) Average experimental temperatures; (—) predicted temperatures by using the finite element software COMSOL. *Freezing conditions*: (a) $T_i = 8.8\,°C$, $T_{ext} = -40\,°C$, position of the thermocouple $x = 0.015$ m, $y = 0.01$ m. (b) $T_i = 12\,°C$, $T_{ext} = -35.4\,°C$, position of the thermocouple $x = 0.018$ m, $y = 0.010$ m. In both experiments $h_{p\text{-}air} = 20\,W/m^2\,K$, $h_{b\text{-}p} = 500\,W/m^2\,K$. Error bar on the top of the figures represents the standard error of the mean experimental temperatures.

data and the temperature evolution obtained by the numerical solutions. The root mean square error (RMSE), was 1.5 °C and the Maximum absolute deviation (MAD) was 3.68 °C. As can be seen from the results there is a very good agreement between experimental and predicted values by using the numerical model for the pouches.

The lack of a marked plateau region in the time–temperature curve in the center of the pouch is not related to the sensor used to record the temperature evolution. As the pouch system has asymmetrical boundary conditions (one side is in contact with the metal plate and the other with the cooling air) the warmest point of the foodstuff is not located at the center of the pouch, and does not maintain a fixed position. The plateau region that clearly defines where the phase change takes place, is strongly dependent on how fast the heat flux penetrates into the food. When the freezing rate increases the plateau region becomes shorter and it takes less time to complete the phase change and surpass the freezing temperature. The Fig. 6b shows the time–temperature predictions for four different positions in the pouch system: X1 = 0 m, X2 = 0.0057 m, X3 = 0.0125 m, and X4 = 0.0170 m, being T1, T2, T3, and T4 the corresponding temperature predictions for X1, X2, X3, and X4. As can be seen the positions which are further away from the metal plate show a marked plateau region since freezing rate is slower compared with the positions closer to the bottom side that is in contact with the metal plate.

With reference to the model validation in crab claws Fig. 7a and b show two examples of the average experimental temperatures vs. time and the predicted curves. The conditions of Fig. 7a were: $T_i = 8.8\,°C$, $T_{ext} = -40\,°C$ and the position of the thermocouple $x = 0.015$ m, $y = 0.010$ m and for Fig. 7b $T_i = 12\,°C$, $T_{ext} = -35.4\,°C$; the position of the thermocouple was $x = 0.018$ m, $y = 0.010$ m. Each test was conducted in triplicates and the standard error of the mean experimental temperatures was represented by the error bar on the top of Fig. 7a and b.

For the experiment shown in Fig. 7a RMSE = 1.5 °C and MAD = 3.65 °C, and for the experiment shown in Fig. 7b RMSE = 0.99 °C and MAD = 2.65 °C. The surface heat transfer coefficients used in the numerical model were $h_{p\text{-}air} = 20\,W/m^2\,K$ and $h_{b\text{-}p} = 500\,W/m^2\,K$. As can be seen, a very good agreement was achieved between model prediction and experiments over the entire freezing period in the case of crab claws.

Table 1 – Effects of surface heat transfer coefficients h'_{p-a} (pouch-air) (W/m^2 K) and external temperatures (T_{ext}) on freezing times of pouches containing crab meat considering $T_i = 7\,^\circ$C and a final temperature of $-15\,^\circ$C.

T_{ext} (°C)	Freezing times (min) in pouches containing crab meat		
	5	10	15
−20	78.0	71.3	65.8
−30	45.8	41.8	38.6
−40	32.6	29.8	27.6

It is important to note that the maximum absolute difference (MAD), which is one of the most important parameter on a numerical algorithm, was in all the experiments (for pouches and crab claws) lower than 4 °C. This implies that that the numerical models can predict freezing times as well as reproduce time–temperature curves in the foodstuff in an accurate manner.

Fig. 8a shows the temperature distribution in the crab claw after 15 min inside the tunnel freezer and Fig. 8b shows the temperature distribution inside the crab claw at different residence times (15, 25, and 30 min) in the tunnel freezer for the indicated operating conditions: $T_i = 8.8\,^\circ$C, $T_{ext} = -20\,^\circ$C, $h_{p\text{-}air} = 20$ W/m^2 K, and $h_{b\text{-}p} = 500$ W/m^2 K.

4.4. *Effect of operating conditions on freezing times*

Once the numerical models were validated assuring that a good agreement with the experimental data was achieved, they were used to simulate different operating conditions varying the external air temperature and the heat transfer coefficients that depend on fluid velocities. Tables 1 and 2 show the calculated freezing times for pouches and crab claws, respectively. Table 1 shows the times needed for the center point in pouches (Fig. 1b) to reach a final value of $-15\,^\circ$C, being the initial temperature of the product 7 °C and considering different external temperatures and heat transfer coefficients at the interface product-air.

Table 2 shows the freezing times for the point $x = 0.022$ m, $y = 0.017$ m (Fig. 2d) in crab claws to reach a final temperature of $-15\,^\circ$C, being the initial temperature 8.8 °C, considering different external fluid temperatures and surface heat transfer coefficients at the interface product-air.

It can be observed the effects of the heat transfer coefficients and the external fluid temperature on the freezing times to reach a final temperature.

Table 2 – Effects of heat transfer coefficients $h_{p\text{-}a}$ (product-air) (W/m^2 K) and external temperatures (T_{ext}) on freezing times of crab claws considering $T_i = 8.8\,^\circ$C and a final temperature of $-15\,^\circ$C.

T_{ext} (°C)	Freezing times (min) of crab claws			
	5	10	15	20
−20	42	39	36	34
−30	40	36	33	30
−40	38	33	29	27

Table 3 – Tracking of the warmest point during freezing of crab meat pouches. Geometric center of the pouch at $x = 0.0085$ m (for axis position see Fig. 1b).

Time (s)	Position of the warmest point (m)
20–30	0.0091
40–60	0.0102
70–110	0.0113
120–180	0.0125
190–400	0.0136
410–450	0.0147
460–910	0.0136
920–1230	0.0125
1240–1290	0.0136
1300–1750	0.0125
1760–2110	0.0136
2120–2400	0.0147
2410–4800	0.0159

4.5. *Tracking of the maximum temperature in each system*

A very important fact when studying the freezing process is tracking the warmest point of the foodstuff; this can help to establish the minimum residence times in the tunnel and assure that the product has reached its final storage temperature.

It is interesting to note that the warmest points in the pouches and in the crab claws do not remain at fixed positions, describing different paths inside the products.

The warmest point in the pouch that has asymmetric boundary conditions was tracked and Table 3 shows the change of its position with time as the freezing process occurs (see Fig. 1b for reference of the axis position). As can be it moves upward until it stabilizes at $x = 0.0159$ m, however it never reaches the interphase where the boundary is submitted to the cooling air condition.

In the case of claws the change in the position can be attributed to the irregular shape of the claw and the different surface heat transfer coefficients that each type of interface shows (product-air and belt-product). In the example shown in Fig. 8a the warmest point is initially close to the geometric center of the claw ($x = 0.02236$ m $y = 0.01388$ m) and as time elapses it moves upwards and to the right, finally reaching a position at the calcareous surface at $x = 0.03977$ m, $y = 0.01668$ m. This path was observed for the simulation case assuming $h_{p\text{-}air} = 20$ W/m^2 K, an initial temperature of the claw $T_i = 8.8\,^\circ$C, and an external cooling air temperature $T_{ext} = -20\,^\circ$C.

The lowest temperature point was also tracked and it was seen that it remained at a fixed position $x = 0.01933$ m and $y = 0$; this value, as expected, lies in contact with the conveyor belt.

The video shows the simulation of how the warmest point (max marker) in the crab claw moves during the freezing process, considering the following operating conditions $h_{p\text{-}air} = 20$ W/m^2 K, initial temperature of the claw $T_i = 8\,^\circ$C, and external cooling air temperature $T_{ext} = -20\,^\circ$C.

Supplementary data associated with this article can be found, in the online version, at http://dx.doi.org/10.1016/j.fbp.2013.07.012.

4.6. *Effect of freezing rates on ice crystal sizes*

Fig. 9a and b show the effect of different freezing rates in the tunnel, operating at different air temperatures and velocities,

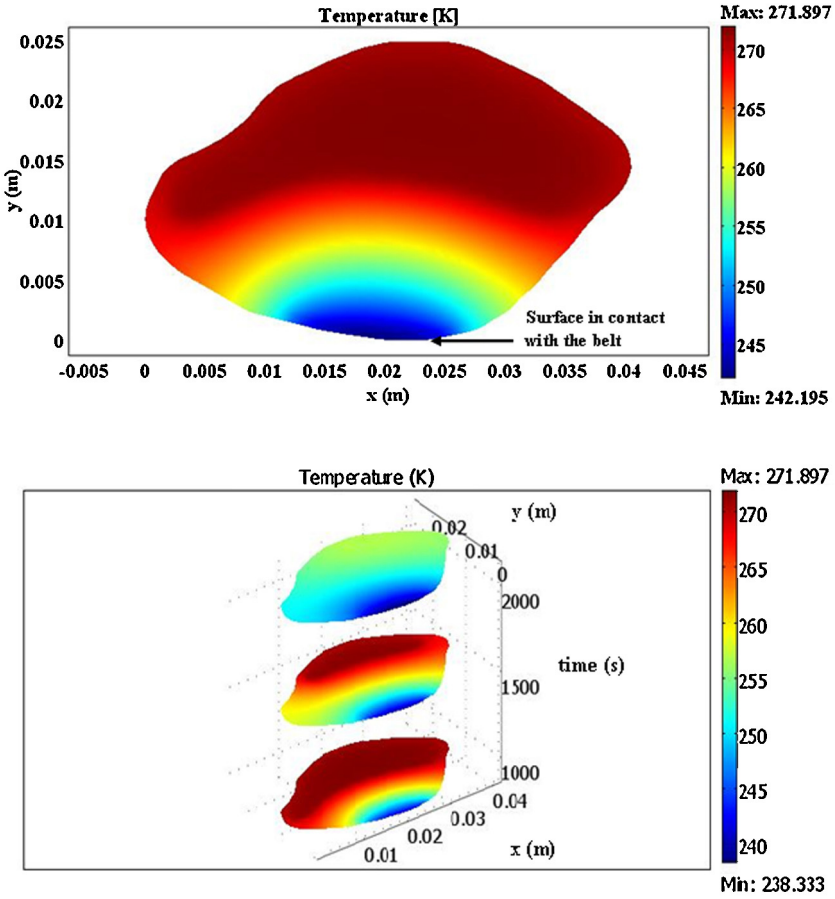

Fig. 8 – (a) Temperature distribution in the claw, after 15 min inside the tunnel freezer. (b) Temperature distributions in a claw after 15, 25, and 30 min inside the tunnel freezer. *Freezing conditions*: $T_i = 8.8\,^{\circ}C$, $T_{ext} = -20\,^{\circ}C$, $h_{p\text{-}air} = 20\,W/m^2\,K$, $h_{b\text{-}p} = 500\,W/m^2\,K$.

on the microstructure of the frozen tissue and the location of the ice crystals. Fig. 9a, shows small intracellular ice crystals with an average ice crystal equivalent diameter of $15 \pm 2\,\mu m$; the micrograph corresponds to a crab meat tissue frozen with a value of air temperature of $-40\,^{\circ}C$, and air velocity 4.16 m/s leading to a local characteristic freezing time of $tc = 11$ min. In Fig. 9b the observed crystals are larger in diameter ($62 \pm 4\,\mu m$) and the corresponding characteristic freezing time was to 29 min (lower freezing rate). The conditions of Fig. 9b were achieved with an air temperature of $-27\,^{\circ}C$ and air velocity of 3.64 m/s. As can be observed freezing rates have notorious influence on ice crystal sizes in the frozen crabs affecting the microstructure of the meat tissue; higher freezing rates (lower tc) led to smaller ice crystals.

Freezing rates directly affect the processing times which influence the size of the ice crystals in the foodstuff. As the freezing times increase, larger ice crystals are obtained which in turn affect the water holding capacity increasing the exudate production. These results will be related in future works, to quality attributes of the product.

4.7. *Simple equations based on numerical simulations to determine the effect of heat transfer coefficients and external temperature on freezing times*

Based on the data shown in Tables 1 and 2 and using a forward stepwise method in SYSTAT 12, polynomial regressions were obtained for plastic pouches and crab claws in order to predict freezing times to reach $-15\,^{\circ}C$ in the warmest points as functions of the external refrigerant air temperature in the tunnel (T_{ext}, °C) and the heat transfer coefficient (air-product) h ($W/m^2\,K$). An excellent agreement between the freezing times estimated by the finite element method and the freezing times estimated by the polynomial equations (FT = Freezing Times) (Eqs. (25) and (26)) was observed. The obtained equations and the corresponding R^2 values are:

For crab meat packed in plastic pouches, $-40\,^{\circ}C \le T_{ext} \le -20\,^{\circ}C$, and $5 \le h'_{p-a} \le 15\,W/m^2\,K$

$$FT(\text{min}) = 202.6 + 7.715(T_{ext}) - 1.893(h'_{p-a}) + 0.088(T^2_{ext})(h'_{p-a}) - 0.036(h'_{p-a})(T_{ext}) \quad (25)$$

with $R^2 = 0.99982$.

For crab claws $-40\,^{\circ}C \le T_{ext} \le -20\,^{\circ}C$, and $5 \le h_{p\text{-}a} \le 20\,W/m^2\,K$:

$$FT(\text{min}) = 46.35 + 0.0478(T_{ext}) - 0.0139(h^2_{p-a}) + 0.0354(T_{ext})(h_{p-a}) - 0.00102(h^2_{p-a})(T_{ext}) \quad (26)$$

with $R^2 = 0.99925$.

These equations constitute simple tools that can be industrially applied to assess the effects of h and external temperature on freezing times with an absolute error in the predicted time lower than 0.5 min.

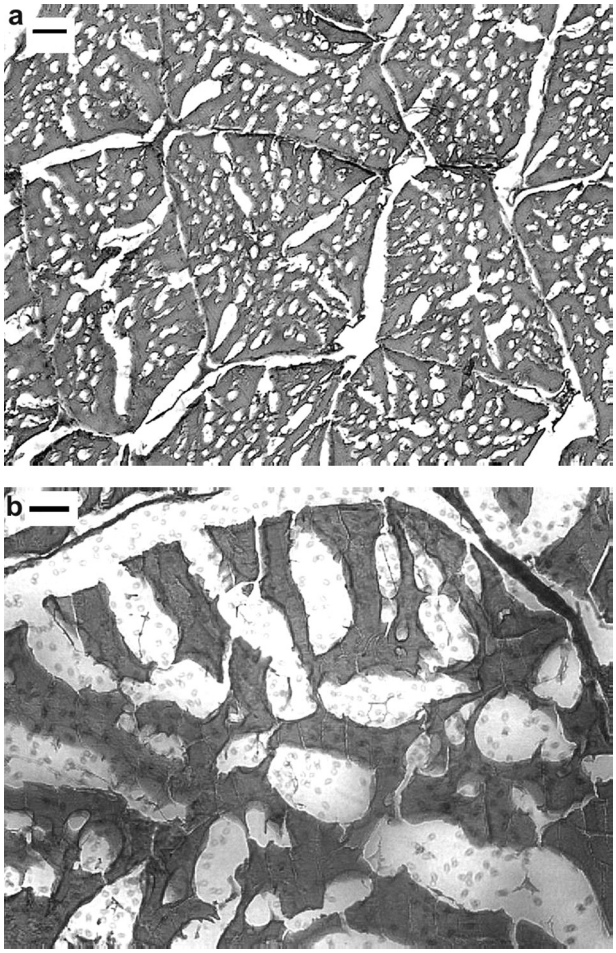

Fig. 9 – Micrographs of crab tissue frozen at different rates represented by the local characteristic freezing time (tc); (a) tc = 11 min; bar represents 100 μm; (b) tc = 29 min; bar represents 50 μm.

5. Conclusions

The freezing of products such as crab claws and meat pouches from unexploited resources of Patagonian marine crabs was experimentally carried out and mathematically modeled. A finite element program coded by the authors was developed using Matlab language; it allowed the prediction of temperature versus time curves during the freezing process of crab meat packaged in pouches. The freezing process of crab claws was numerically modeled considering two relevant aspects: the thermal resistances in series (calcareous layer and crab meat) and the irregular shape of the claws.

The numerical models included experimental heat transfer coefficients, determined in the industrial tunnel freezers. Thermo-physical properties measured by Differential Scanning Calorimetry, and estimated by predictive equations that take into account the ice fraction as a function of temperature in the foodstuff were introduced in the model.

The numerical predictions were contrasted with experimental freezing times showing an excellent agreement. The models were applied to predict freezing times in a fast and accurate manner. Tracking of the warmest points during freezing of pouches and claws were performed.

The influence of the freezing rate on the size and location of the ice crystals in the tissue was determined by histological observations.

The effects of heat transfer coefficients and external fluid temperature on freezing times of claws and pouches were also determined by using the numerical model and were finally represented by simple polynomial equations that can easily be used in the industry.

All the obtained information is of great value for food process design and can help to optimize and control the freezing of new products.

Acknowledgments

The authors acknowledge the financial support of Universidad Nacional de La Plata, Consejo Nacional de Investigaciones Científicas y Tecnológicas (CONICET), Agencia Nacional de Promoción Científica y Tecnológica (ANPCYT), y CENPAT (Centro Nacional Patagónico-CONICET) ARGENTINA and to Ing. Miguel Galarza, responsible of REFMAR S.R.L. in Puerto Madryn, Chubut. Argentina.

References

Ahmed, J., Rahman, S., 2009. Thermal conductivity data of foods. In: Rahman, M.S. (Ed.), Food Properties Handbook. , 2nd ed. CRC Press/Taylor and Francis Group, Boca Raton/London/New York, pp. 596–601 (Chapter 18).

Alvarez, I., Briquets, V., 1983. Resultados de los estudios de morfometría y regeneración del cangrejo moro (*Menippe mercenaria*) en el Golfo de Batabanó, Cuba. Rev. Cub. Inv. Pesq. 8, 64–77.

AOAC, 1990. Official Methods of Analysis, vol. 2., 15th ed. Association of Official Analytical Chemists, Inc., Arlington.

ASTM Standard E1269 – 05 Standard Test Method for Determining Specific Heat Capacity by Differential Scanning Calorimetry, ASTM, International, West Conshohocken 2003 PA, DOI: 10.1520/E1269-05, www.astm.org

Bevilacqua, A.E., Zaritzky, N.E., Calvelo, A., 1979. Histological measurements of ice in frozen beef. J. Food Technol. 14, 237–251.

Bevilacqua, A.E., Zaritzky, N.E., 1980. Ice morphology in frozen beef. J. Food Technol. 15, 589–597.

Brigaud, F., Vasseur, G., 1989. Mineralogy, porosity and fluid control on thermal conductivity of sedimentary rocks. Geophys. J. Int. 98 (3), 525–542.

Carson, J.K., 2006. Review of effective thermal conductivity models for foods. Int. J. Refriger. 29, 958–967.

Choi, Y., Okos, M.R., 1986. Effects of temperature and composition on the thermal properties of foods. In: Le Maguer, M., Jelen, P. (Eds.), Food Engineering and Process Applications 1. Elsevier Applied Science, New York, pp. 93–103.

Codex Alimentarius Commission CAC/RCP, 1983. Recommended International Code of Practice for Crabs, Rome, vol. 9. p. 28.

Comini, G., Del Giudice, S., Lewis, R.W., Zienkiewicz, O.C., 1974. Finite element solution of non-linear heat conduction problems with special reference to phase change. Int. J. Numer. Methods Eng. 8, 613–624.

Dima, J.B., Barón, P.J., Zaritzky, N.E., 2012. Mathematical modeling of the heat transfer process and protein denaturation during the thermal treatment of Patagonian marine crabs. J. Food Eng. 113, 623–634.

Edwards, E., Early, J., 1976. Catching handling and processing crabs. Torry Advisory Notes, 26. Torry Research Station, pp. 3–17.

Erdogdu, F., 2010. Fundamental of heat transfer in food processing. In: Farid, M. (Ed.), Mathematical Modeling of Food Processing. CRC Press/Taylor and Francis Group, Boca Raton, FL, pp. 69–88 (Chapter 3).

FAO Capture Production 1950–2009, 2009. Fisheries Department, Fisheries Information, Data and Statistic Unit. Fishstat Plus. Universal Software for Fisheries V 2.3.

Fennema, O.R., Powrie, W.D., Marth, E.H., 1973. Low Temperatures Preservation of Foods and Living Matter. Marcel Dekker Inc., New York.

Fenucci, J.L., Boschi, E.E., 1975. Contribución al conocimiento biológico del cangrejo comercial de las aguas costeras de la provincia de Buenos Aires *Ovalipes trimaculatus* (De Haan) (Crustacea, Decapoda, Portunidae). Phys. Sect. A 34. (89), 291–308.

Gates, K., Parker, A.H., Bauer, D.L., Wen Huang, Y., 1993. Storage changes of fresh and pasteurized Blue Crab meat in different types of packaging. J. Food Sci. 58 (2), 314–317.

Green, D.W., Perry, R., 2007. Perry's Chemical Engineers' Handbook, 8th ed. Mc-Graw Hill, New York.

Kolbe, E., Kramer, D.E., 2007. Planning for Seafood Freezing. Alaska Sea Grant College, Fairbanks, Alaska, pp. 50–59.

Jacobs, J.K., Kerrick, D.M., Krupka, K.M., 1981. The high temperature heat capacity of natural calcite ($CaCO_3$). Phys. Chem. Miner. 7, 55–59, Springer Verlag.

Leal, G.A., Dima, J.B., Dellatorre, F.G., Barón, P.J., 2008. Schedule of the reproductive events and maturity at size of the Patagonian stone crab *Platyxanthus patagonicus* (Brachyura, Platyxanthidae). J. Crust. Biol. 28 (2), 262–269.

Mannapperuma, J.D., Singh, R.P., 1988. Prediction o freezing and thawing times of foods using a numerical method based on enthalpy formulation. J. Food Sci. 53, 626–630.

Mannapperuma, J.D., Singh, R.P., 1989. A computer-aided method for prediction of properties and freezing/thawing times of foods. J. Food Eng. 9, 275–304.

Martino, M.N., Zaritzky, N.E., 1989. Ice recrystallization in a model system and in frozen muscle tissue. Cryobiology 26, 138–148.

McNaughton, J.L., Mortimer, C.T., 1975. Differential Scanning Calorimetry. Perkin Elmer Corporation, Connecticut, USA.

Meyers, M.A., Chen, P.Y., Lin, A.Y.M., 2008. Biological materials: structure and mechanical properties. Prog. Mater. Sci. 53, 1–206.

Midttomme, K., Roaldset, E., Aagaard, P., 1998. Thermal conductivity, claystones and mudstones of selected from England. Clay Miner. 33, 131–145.

Miles, C.A., Van Beek, G., Veerkamp, C.H., 1983. Calculation of the thermophysical properties of foods. In: Jowitt, R., et, al. (Eds.), Physical Properties of Foods. Appl. Sci. Publ., London, England, pp. 269–312.

Neeper, D.A., 2000. Thermal dynamics of wallboard with latent heat storage. Solar Energy 68 (5), 393–403.

Oshiro, L.M., 1999. Aspectos reprodutivos do caranguejo guaia, *Menippe nodifrons* Stimpson (Crustacea: Decapoda: Xanthidae) da Baia de Sepetiba, Rio de Janeiro, Brasil. Rev. Bras. Zool. 16, 827–834.

Pham, Q.T., 2012. Mathematical modeling of freezing processes. In: Sun, D.W. (Ed.), Handbook of Frozen Food Processing and Packaging. , 2nd ed. CRC/Taylor and Francis Group, Boca Raton/London/New York, pp. 147–186 (Chapter 7).

Pham, Q.T., 2008. Modelling of freezing processes. In: Evans, J. (Ed.), Frozen Food Science and Technology. Blackwell Publishing, Oxford, England.

Purlis, E., 2011. Bread baking: technological considerations based on process modeling and simulation. J. Food Eng. 103, 92–102.

Roos, Y.H., 1986. Phase transitions and unfreezable water content of carrots, reindeer meat and white bread studied using differential scanning calorimetry. J. Food Sci. 51 (3), 684–686.

Santos, M.V., Lespinard, A., 2011. Numerical simulation of mushrooms during freezing using the FEM and an enthalpy: Kirchhoff formulation. Heat Mass Transfer 47, 1671–1683.

Santos, M.V., Vampa, V., Califano, A., Zaritzky, N., 2010. Numerical simulations of chilling and freezing processes applied to bakery products in irregularly 3D geometries. J. Food Eng. 100, 32–42.

Scheerlinck, N., Fikiin, K.A., Verboven, P., De Baerdemaeker, J., Nicolaï, B.M., 1997. Solution of phase change heat transfer problems with moving boundaries using an improved finite element enthalpy method. In: Van Keer, R., Brebbia, C.A. (Eds.), Moving Boundaries IV: Computational Modelling of Free and Moving Boundary Problems. , pp. 75–85.

Scheerlinck, N., Verboven, P., Fikiin, K.A., De Baerdemaeker, J., Nicolaï, B.M., 2001. Finite element computation of unsteady phase change heat transfer during freezing or thawing of food using a combined enthalpy and Kirchhoff transform method. Trans. ASAE 44 (2), 429–438.

Thoma, B.P., Peter, K.L., Felder, D.L., 2012. Review of the family Platyxanthidae Guinot, 1977 (Crustacea, Decapoda, Brachyura, Eriphioidea), with the description of a new genus and a key to genera and species. Zootaxa 3498, 1–23.

Wang, L., Curtis, W., 2012. Thermophysical properties of frozen foods. In: Da Wen Sun (Ed.), Handbook of Frozen Food Processing and Packaging. , 2nd ed. CRC Press/Taylor and Francis Group, Boca Raton/London/New York, p. 117 (Chapter 5).

Zaritzky, N.E., 2000. Factors affecting the stability of frozen foods. In: Kennedy, C.J. (Ed.), Managing Frozen Foods. Woodhead Publishing Limited, Cambridge, England, pp. 111–133.

Zaritzky, N.E., 2011. Physical–chemical principles in freezing. In: Sun, D.W. (Ed.), Handbook of Frozen Food Processing and Packaging. , 2nd ed. CRC Taylor/Francis Group, Boca Raton/London/New York, pp. 3–38 (Chapter 1).